Brodogradnja/Shipbuilding/Open access Volume 74 Number 3, 2023

Ahmad Irham Jambak
Ismail Bayezit

http://dx.doi.org/10.21278/brod74307

ISSN 0007-215X
eISSN 1845-5859

Robust optimal control of a nonlinear surface vessel model with parametric uncertainties

UDC 629.56:005.591.1
Original scientific paper

Summary

This paper presents a fast alternative optimization method for developing a reliable optimal controller that can handle system model parameter uncertainties. The source of uncertainty in this study is identified as hydrodynamic coefficients, which are prone to errors due to the challenges involved in obtaining accurate values. The proposed optimization method utilizes a complex nonlinear ship model provided by Maneuver Modelling Group (MMG) as the reference for the ship motion model. The optimization process is divided into two stages: a blind search followed by bisection optimization, to obtain a robust optimal controller. To demonstrate the effectiveness of the proposed approach, system response analysis and practical tests were performed on Step, M-Turn, and Doublet maneuvers. The results show that the controller parameters obtained from the proposed optimization method are capable of achieving high success rates in controlling a system with uncertain parameters.

Key words: *robust control; optimal control; optimization; parametric uncertainty; autonomous surface vessel, autonomous marine vehicle*

1. Introduction

The automation of ship control has revolutionized the shipping industry, improving efficiency, reducing costs, and enhancing safety. Automated ship control includes functions such as steering, propulsion, and monitoring of critical equipment, and has made it possible to remotely control or monitor ships from shore, reducing the number of crew members required on board [1]. One of the critical factors in ship design, performance, and manoeuvring is the hydrodynamic coefficient [2]. These coefficients represent the forces and moments acting on the vessel's hull, rudder, and propeller, which are essential for predicting the ship's motion and stability [3]. Unfortunately, hydrodynamic coefficients are not always accurate due to factors such as the vessel's speed, sea conditions, and changes in the vessel's geometry and loading [4]. As a result, it can be challenging to determine hydrodynamic coefficients accurately, making it difficult to control the vessel's motion and stability.

Numerous studies have been conducted in the field of controlling ship with hydrodynamic coefficients with uncertainties associated with them. Several approaches have been used, including predictive methods such as Multi-level Model Predictive Control (MPC), which was

proposed by Haseltalab et al. [5] to control ship speed and calculate propulsion energy in the presence of uncertainties. Another method involves the use of adaptive control, as pursued by Lu et al. [6], which involves continuously adjusting control inputs based on real-time ship behaviour measurements. Fuzzy logic-based control has also been implemented, as seen in the work carried out by Chen and Tan [7], where the ship's control inputs are adjusted based on fuzzy rules that take into account uncertainty in hydrodynamic coefficients. Additionally, machine learning-based approaches have been used, such as the reinforcement learning method employed by Zhang et al. [8] to adjust the ship's control inputs based on given data. Another technique, robust control, is designed to maintain stable and predictable ship behaviour even in the presence of uncertain hydrodynamic coefficients, as demonstrated by Ye et al. [9].

The focus of this study to implement a robust controller for the aforementioned problem. Robust controllers employ a mathematical model that considers uncertain parameters [10] to handle the possible range of values for those parameters. This type of controller ensures that the vessel remains stable and operates correctly under various conditions [11]. However, finding a suitable robust controller can be challenging using deterministic methods like linear or nonlinear approach [12]. For instance, the commonly used ship motion model provided by the Maneuvering Modelling Group (MMG) has 17 coefficients for the hull's hydrodynamic coefficient alone, making the optimization problem complex and large [13]. To address this issue, optimization techniques such as Particle Swarm Optimization (PSO) and Genetic Algorithms (GA) [14-16] have been used to determine the optimal coefficients that best match the ship's motion. However, these methods can be slow, particularly if a large number of samples [17] are needed to represent the uncertainties in the hydrodynamic coefficients.

To address this limitation, this study aims to design and test a faster optimization algorithm to handle large and complex optimization problems such as those associated with ship hydrodynamic coefficients. First, the problem mathematically formulated in Section 2 where the slow performance of existing methods such as PSO and GA is investigated. Section 3 introduces designed optimization method namely Bisection Optimization via Blind Search, which is faster compared to the other mentioned methods. Section 4 presents the optimization properties and results. Additional 3 test cases: Step, M-Turn, and Doublet maneuver, discussed in Section 5 to further test the obtained controller parameters. This paper finalized with conclusions presented in Section 6.

2. Problem Formulation

Consider following hydrodynamic force equations acting on ship hull provided by MMG [13]:

$$X_H = \frac{\rho L_{pp} d U^2 X'_H(v'_m, r')}{2} \tag{1}$$

$$Y_H = \frac{\rho L_{pp} d U^2 Y'_H(v'_m, r')}{2} \tag{2}$$

$$N_H = \frac{\rho L_{PP}^2 d U^2 N'_H(v'_m, r')}{2} \tag{3}$$

where X_H, Y_H and N_H are surge force, sway force and moment acting on the ship hull while prime accents denote nondimensionalized unit of measurements that represent following polynomials:

$$X'_H(v'_m, r') = -R'_0 + X'_{vv} v'^2_m + X'_{vr} v'_m r' + X'_{rr} r'^2 + X'_{vvvv} v'^4_m \tag{4}$$

$$Y'_H(v'_m, r') = Y'_v v'_m + Y'_R r' + Y'_{vvv} v'^3_m + Y'_{vvr} v'^2_m r' + Y'_{vrr} v'_m r'^2 + Y'_{rrr} r'^3 \tag{5}$$

$$N'_H(v'_m, r') = N'_v v'_m + N'_R r' + N'_{vvv} v'^3_m + N'_{vvr} v'^2_m r' + N'_{vrr} v'_m r'^2 + N'_{rrr} r'^3 \quad (6)$$

here, all of the subscripted *X*, *Y*, and *N* on the right-hand side of Eq. (4) to Eq. (6) are the hydrodynamics coefficients $\vartheta \in \Theta$.

Conventional way of treating these 17 parameters is by defining them as a fixed coefficient which obtained through experimental results or computational fluid dynamics (CFD) analysis [13] resulting a fixed polynomial. In this case, controlling such deterministic model is not a challenging task as there are numerous available studies that cover the topic of nonlinear control. However, as mentioned in Section 1, the estimation of hydrodynamic coefficients can be associated with a degree of inaccuracy. Therefore, even if a controller is designed and performs well in simulation, the performance in a real-world scenario may be affected by these inaccuracies. Indeed, if all parameters being considered as uncertain variable finding optimal controller deterministically will involve complex mathematical calculations [18]. In such cases, metaheuristic optimization approaches such as Particle Swarm Optimization (PSO) and Genetic Algorithm (GA) are commonly used [19]. To employ these methods, a desired cost ω_d defined and search for a controller parameter *K* value that results in a cost ω less than the desired cost [20]. This optimization problem can be formulated as follows:

$$\omega_d \geq \omega(\vartheta, K) \quad (7)$$

where the cost ω given $\vartheta \in \Theta$ and *K* has to be less than ω_d. However, due to the fact that $\vartheta \in \Theta$ are generally comes with some degree of error [21], ϑ obtained from experimental result or CFD analysis defined as the nominal parameter ϑ_0 while highest and lowest possible value of ϑ has to be introduced as follows:

$$\Theta \triangleq \{\vartheta \in [\vartheta^-, \vartheta^+]; \vartheta^- \leq \vartheta_0 \leq \vartheta^+\} \quad (8)$$

here, ϑ^- and ϑ^+ denote lower bound and upper bound of ϑ_0. To be able to have a controller that can also compensate these uncertainties, controller obtained from Eq. (7) will not be sufficient. Instead, we need to have a robustness problem synthesized to the equation. This can be expressed as follows:

$$\omega_d \geq \{\omega(\vartheta, K) \; \forall \; \vartheta \in \Theta\} \quad (9)$$

As previously mentioned, typically optimization problem from Eq. (7) solved by using metaheuristic optimization algorithm [22] due to the complexity of the MMG model. This optimization algorithm is commonly used to find optimal solutions for complex problems where traditional optimization methods are not effective [23]. While metaheuristic method such as GA and PSO have been shown to be effective at solving such problems expressed by Eq. (7), with large number of uncertain variables being introduced, they can be computationally expensive. Fig. 1 illustrates how PSO or GA would work given uncertainties problem:

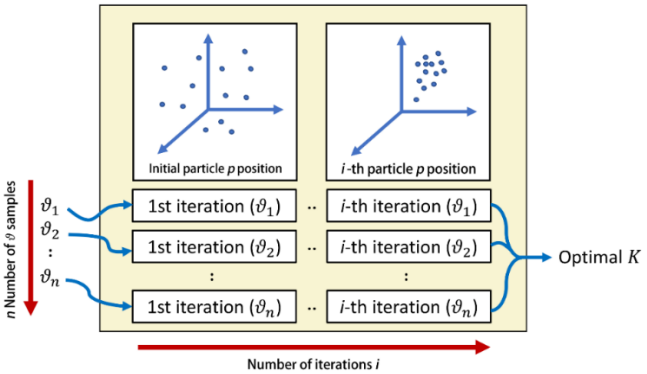

Fig. 1 Particle or Population Based Optimization for Multi-sample Problem

For every sample of the model ϑ, the motion model is simulated with p number of particles for i iterations. Meaning, the number of motion model together with the control algorithm being simulated ϖ can be expressed as follow:

$$\varpi_{PSO/GA} = n.p.i_{PSO/GA} \tag{10}$$

As we increase the number of samples ϑ set of $[\vartheta^-, \vartheta^+]$, number of particles p, and iteration $i_{PSO/GA}$ to be dense enough in order to obtain desired accuracy [24], we significantly increase the number of models being simulated which corresponds to amount of time needed to perform the optimization process. Assume that the time taken for finding an optimal K to satisfy Eq. (7) is 20 hours. Then for 10,000 samples ϑ set of Θ, we are expecting 200,000 hours or approximately 25 years to solve problem from Eq. (8) with the same optimization algorithm. Here we can see that the existence of solution in this case is necessary but not sufficient considering the time taken to run the simulation is also an important factor. The solution of this problem requires both good result as well as reasonable amount of time to run the optimization simulation.

3. Bisection Optimization via Blind Search

In this section, we present an approach for optimizing the problem introduced in Section 2. Bisection Optimization via Blind Search is a two-step optimization algorithm that utilizes a blind search technique in the first stage, followed by a refinement process using the bisection method to obtain the optimal controller. The steps involved in this method described in Fig. 2.

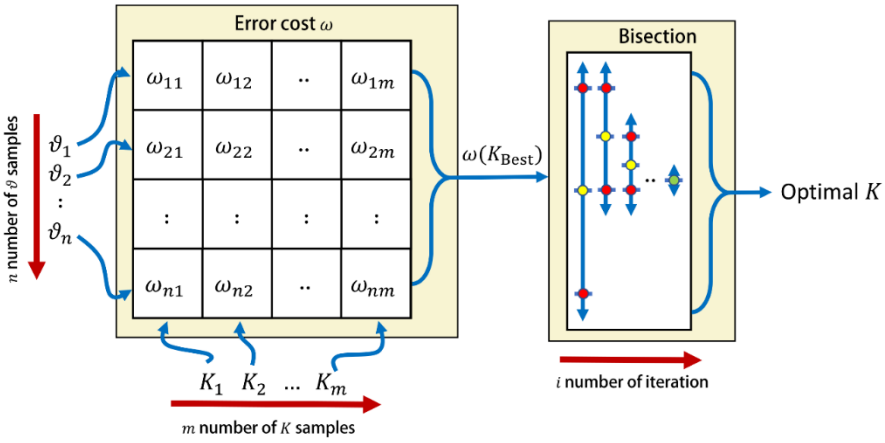

Fig. 2 Bisection Optimization via Blind Search for Multi-sample Problem

In this approach, the model is simulated for n samples, using m sampled controller parameters K, and saving the resulting cost value ω. The controller parameter K, that yields the lowest value of ω is then refined in the second stage using a bisection-based optimization method. The number of simulations of the motion model and control algorithm need to be completed, denoted by ϖ, can be expressed as follows:

$$\varpi_{BB} = n.m + n.i_{BB} = n(m + i_{BB}) \tag{11}$$

Here we can see that the number iteration of bisection method i_{BB} has additive relation to the number of K samples m compared to $i_{PSO/GA}$ which multiplicatively effects to ϖ. Hence, the proposed algorithm can significantly reduce the optimization time.

3.1 Methods of sampling

As mentioned in the problem formulation, the hydrodynamics coefficients are the uncertain parameter in this study. A Gaussian distribution employed for random generation to

account for uncertainties in the model. The reason for choosing this distribution is to treat the hydrodynamics coefficient obtained from experimental results as a valid reference for the model uncertainties. As explained in Section 2, the uncertainty range is defined as:

$$\vartheta^- \leq \vartheta_0 \leq \vartheta^+ \tag{12}$$

Where the mean of the distribution will be based on the nominal sample ϑ_0, while the standard deviation of the distribution will determine the level of error associated with the hydrodynamics coefficient. The distribution of model uncertainties and the impact of standard deviation on its shape are visually illustrated in Fig. 3.

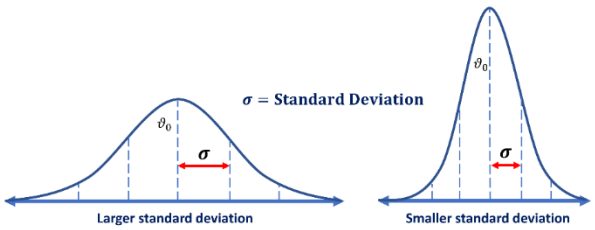

Fig. 3 Gaussian-based sampling of model uncertainties

The number of samples required to obtain a reliable estimate of real-world scenarios will be determined using a function introduced by Lyonett and Toscano [25], which is expressed as follows:

$$n \geq \frac{\ln(1-a)}{\ln(1-b)} \tag{13}$$

The minimum number of samples required for a reliable estimate is denoted as *n*, with *a* and *b* being parameters that determine the level of confidence in the sampling method. The value of *a* and *b* ranges from 0 to 1, with a larger value of *a* resulting in a greater number of samples needed, and a larger value of *b* requiring fewer samples.

In contrast to the sampling of model uncertainties, the controller parameters *K* are randomly generated using a uniform distribution, as there is no prior information about the optimal controller [26]. The process involves specifying the search interval and the required number of samples. The value of *n* obtained from Eq. (13) is used to determine the number of *K* samples.

3.2 Performance criterion

The evaluation of a controller's performance during the optimization process conducted through the use of a cost function. Four distinct types of error-based cost functions *J* are considered, namely: Integral of Absolute Error (IAE); Integral of Squared Error (ISE); Integral of Time multiplied Absolute Error (ITAE); and Integral of Time multiplied Squared Error (ITSE). Table 1 shows mathematical expressions and descriptions of all mentioned functions.

Table 1. Cost functions and respective equations.

Cost Function	Equation
IAE	$J_{\text{IAE}} = \int \lvert e \rvert dt$
ISE	$J_{\text{ISE}} = \int e^2 dt$
ITAE	$J_{\text{ITAE}} = \int t\lvert e \rvert dt$
ITSE	$J_{\text{ITSE}} = \int te^2 dt$

IAE measures the steady-state error of a control system by minimizing the integral of the absolute error over time [27,28]. Similarly, ISE minimizes the integral of the squared error over time, making it suitable for evaluating the steady-state error of a control system [27,28,30]. ITAE, on the other hand, is designed to minimize the integral of the absolute error over time while prioritizing fast and accurate response times [27]. This cost function is commonly used in systems that require quick and precise responses [27,29]. Finally, ITSE computes the integral of the absolute error over time, making it suitable for systems that require fast and accurate response times but may be more sensitive to overshoot or oscillation [26,28,30].

4. Simulation Results

A simulation scenario created where the controller is given a task of changing the yaw angle ψ, from 0 degree to 40 degree. To evaluate the effectiveness of the controller, the study introduced varying levels of uncertainty to assess its ability at maintaining stability with tolerable variations in the system parameters. In this paper, the levels of uncertainty considered to be ±20% which represent the extent to which the parameters can deviate from their nominal values.

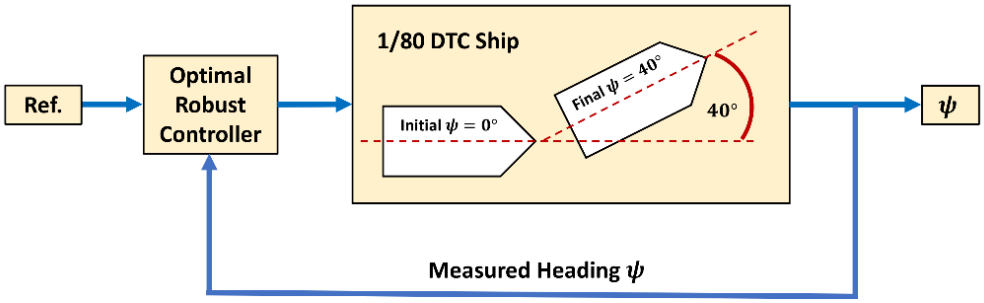

Fig. 4 Heading angle ψ control optimization

Fig. 4 illustrates the scenario for the optimization. The output Optimal Robust Controller block is rudder angle δ which has angle saturation max. 35 degree and turning rate saturation of max. 10 degrees/second. The ship has initial surge speed 1.179 m/s and the propeller speed is 5 revolutions/second.

In this study, two types of controllers were investigated, namely proportional (P) and proportional-derivative (PD) controllers. The justification of derivative term inclusion is to damp out oscillations or overshoot in the system's response which can improve the stability and settling time [23]. On the other hand, the integral term considered to be excluded due to the system's inherent stability [27] and expected slow response.

The relation between controller parameters and input of the system δ can be expressed as follow [32]:

$$\delta_P = K_P(\psi_{\text{ref}} - \psi_{\text{meas}}) \tag{18}$$

$$\delta_{PD} = K_P(\psi_{\text{ref}} - \psi_{\text{meas}}) + K_D[(\psi_{\text{ref}} - \psi_{\text{meas}}) - (\psi_{\text{ref,prev}} - \psi_{\text{meas,prev}})] \tag{19}$$

where P-controller input δ_P is the multiplication of proportional gain K_P and the difference between heading angle reference ψ_{ref} and current measured heading angle ψ_{meas}. In the case of PD-controller, the input equation has additional term which is the multiplication of derivative gain K_D and the difference between current and previous error.

4.1 Optimization parameters

The scaled 1/80 DTC ship model was chosen for simulation in this study due to the ease of accessibility and availability of its parameters. Table 2 provides a list of the parameters to run the simulation of MMG ship motion model. All of the symbols used are using the parameter from MMG model paper [13] and the derivation of the equations are not discussed in this paper.

Table 2. Geometric Properties and Hydrodynamic Coefficients of 1/80 DTC Ship

Geometric Properties	L	m	I_z	x_g		
	7	3.27	0.2044	0.011		
Hull Hydrodynamic Coefficients	R_0	X_{vv}	X_{vr}	X_{rr}	X_{vvvv}	
	-0.033	-0.0491	-0.1201	-0.0509	0	
	Y_v	Y_r	Y_{vvv}	Y_{vvr}	Y_{vrr}	Y_{rrr}
	-0.3579	0.127	-0.2509	0.1352	0	0
	N_v	N_r	N_{vvv}	N_{vvr}	N_{vrr}	N_{rrr}
	-0.0698	-0.0435	-0.0588	-0.0367	0	0
Propeller Hydrodynamic Coefficients	k_0	k_1	k_2	t_P		
	-0.1060	-0.3246	0.4594	0.22		
	D_P	w_{P0}	C_1	$C_2(\beta > 0)$	$C_2(\beta < 0)$	
	2.6	0.35	0	1.6	1.1	
Rudder Hydrodynamic Coefficients	t_R	x_R	f_α	u_R		
	0	-16	2.747	0.5		
	a_H	a_R	$\gamma_R(\beta > 0)$	$\gamma_R(\beta < 0)$		
	0.312	-0.0655	0.640	0.395		

Table 3. Bisection Optimization via Blind Search Properties

Optimization Properties	$S_{1,BB}$	$S_{2,BB}$	d	m	a	b
	0	100	5	10,000	0.995	0.005

All 17 coefficients of the hull hydrodynamic coefficients listed in Table 2 are treated as nominal value of uncertain parameter ϑ_0. Optimization parameters can be seen in Table 3 where 10,000 controller parameter K is sampled with lower search bound $S_1 = 0$ and upper interval bound $S_2 = 100$. The initial bisection interval $d = 5$ and we obtain number of uncertainties sample $n = 1058$ which determined from parameter a and b as shown in Eq. (13).

4.2 Optimization results

The simulation was run on a computer with an Intel Core i7-9750H, 20GB of RAM, an NVIDIA Quadro T1000 graphics card and the simulation software used is MATLAB R2022b. The total elapsed time for each optimization is approximately 15 hours.

Table 4. Optimization Results

Cost Function	**P-controller**		**PD-controller**		
	K_P	**Cost**	K_P	K_D	**Cost**
IAE	2.70	7632.63	1.83	10.30	6684.96
ISE	2.51	3365.27	1.45	11.01	2709.62
ITAE	2.81	69776.19	1.84	10.31	47857.26
ITSE	2.62	15128.92	1.80	10.27	12229.44

Both P and PD-controller has same amount of controller parameter being sampled *m*. The only difference is PD controller has pairs of $K = [K_P, K_D]$, instead of only K_P. The results are listed in Table 4. All error criterion provides practically the same result although the decimals are varied. Cost functions which employ a time multiplicative factor (ITAE and ITSE) demonstrate a slightly larger K_P value compared to IAE and ISE. Nevertheless, the main insight from the table is it can be seen that PD-controller outperformed the P-controller, as lower cost associated with the former. It should be noted that the comparison of costs between different error criterion is not meaningful, since each of them employs a different equation to calculate the error.

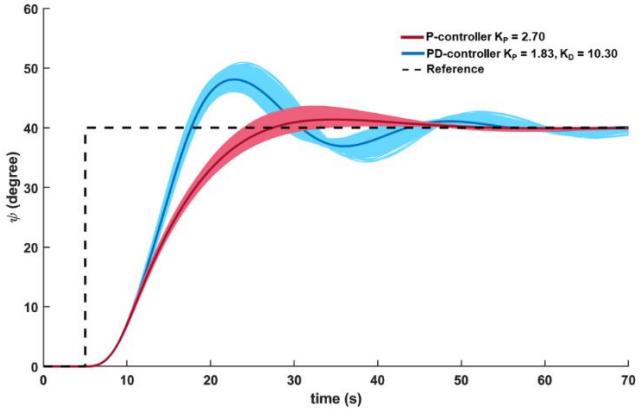

Fig. 5 System responses with P and PD-controller via IAE

In order to visualize the result from Table 4, optimum controller obtained via IAE selected arbitrarily to be plotted in Fig. 5. Darker lines represent the system response in the ideal condition where there are no hydrodynamic coefficients error while the lighter coloured regions are actually a group of densely stacked lines that represents the system response with 1058 random gaussian variation of hydrodynamic coefficient with 20% level of uncertainty. It can be observed that adding derivative term into controller gives a damping effect on the system's response that reduce overshoot and oscillations, resulting in a faster settling time.

4.3 Computational Efficiency Comparison

In this subsection, we compare the computational efficiency of our proposed optimization method with conventional PSO algorithm. The comparison is conducted based on the execution time required to reach the optimal solution with desired tolerance. Note that in Section 2, we discussed the impracticality of conducting PSO optimization for the entire range of sampled uncertainty variation, n = 1058. Therefore, in this simulation, we only consider the nominal value. Table 5 lists PSO optimization parameters.

Table 5. Particle Swarm Optimization Properties

Optimization Properties	$S_{1,PSO}$	$S_{2,PSO}$	N	Stopping criterion	Cost Function
	0	100	100	If $\Delta K_P \leq 0.01$ and $\Delta K_D \leq 0.01$	IAE

Here, a swarm size of N = 100 was employed and the stopping criterion was selected based on the requirement of considering only 2 decimal places, as shown in Table 5. The simulation was conducted only for PD-controller, as P-controller did not yield satisfactory results in the previous section. Again, IAE arbitrarily selected for error criterion as the other three cost functions provide relatively similar results. After 7 iterations which took approximately 19 minutes, K_P = 4.17 and K_D = 9.35 obtained.

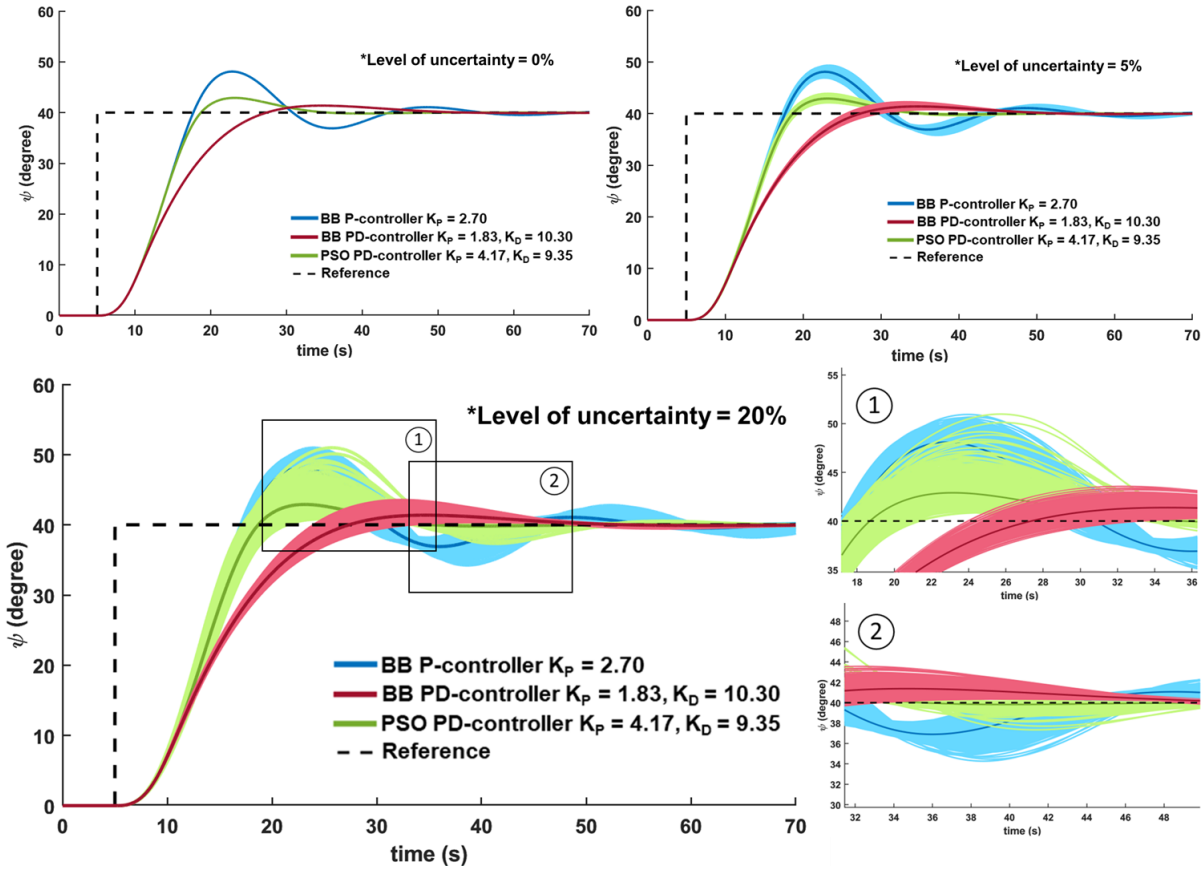

Fig. 6 System responses with P/PD-controller from proposed method and PD-controller from PSO for 0%, 5%, and 20% level of uncertainties.

The obtained controller parameters obtained via PSO algorithm are tested in a same simulation scenario introduced in Subsection 4.2. and the system's responses are compared in Fig. 6. The simulation results demonstrate that in conditions of ideal situations (0%) or low uncertainty (5%), PD-controller from PSO algorithm arguably provides the best performance for ship motion control. Although some small overshoot is observed, the settling time is quicker compared to other methods. However, as the level of uncertainty increases to 20%, undesired behavior starts to appear. For certain combinations of parameter variations, the system response yields 25% overshoot, which is not desirable in ship motion control. In contrast, the PD-controller obtained from Bisection Optimization via Blind Search shows a more stable response and quicker overall settling time in higher uncertainty conditions. This can be attributed to the fact that the PD-controller via our proposed method considers all possible model parameter variations (n = 1058) while the PSO algorithm does not. If all model samples were to be considered in PSO algorithm, the simulation time required would be approximately become 19 minutes x 1058 samples = 22218 minutes, or around 14 days. This shows that our proposed method is 22 times faster.

5. Test Cases

In this section, additional tests conducted to further enhance our comprehension of how well the controllers perform. These tests involved three different scenarios: Step, M-Turn, and Doublet maneuver test. The ship provided with a set of position coordinates in the form of x and y references. The reference coordinates which used the ship's length L as a reference point are listed in Table 6. We varied the locations to see if the control system could handle different scenarios effectively.

Table 6. x and y coordinate references.

Step	$\boldsymbol{x}$ **(***L***)**	0	1	1	3				
	$\boldsymbol{y}$ **(***L***)**	0	0	1	1				
M Turn	$\boldsymbol{x}$ **(***L***)**	0	1	2	3	4			
	$\boldsymbol{y}$ **(***L***)**	0	1	-1	1	0			
Doublet	$\boldsymbol{x}$ **(***L***)**	0	1	1	2	2	3	3	4
	$\boldsymbol{y}$ **(***L***)**	0	0	1	1	-1	-1	0	0

The ship's ability to reach each point is the main objective in this test cases, rather than the specific angle at which it arrives or which path it should follow. Fig. 7 illustrates the control loop for these test cases, which outlines the steps involved in the process.

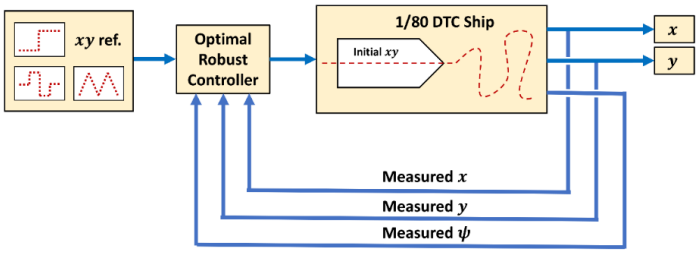

Fig. 7 Waypoint control of 1/80 DTC Ship.

It is apparent that the system references are given in *xy*-coordinates, whereas the input of the system requires heading angle as a reference. Hence, a transformation is necessary to convert the input reference from *xy*-coordinates to a heading angle reference. This can be formulated as follow [32]:

$$\psi_{\text{ref}} = \arctan2\left(\frac{y_{\text{ref}} - y_{\text{meas}}}{x_{\text{ref}} - x_{\text{meas}}}\right) \tag{20}$$

where x_{ref} and y_{ref} are x and y coordinates reference respectively while x_{meas} and y_{meas} are measured coordinates at current time step. The process of feeding input to the controller is done incrementally, one reference point at a time where the ship must be within 50 cm of the current reference point before the next reference point can be tracked.

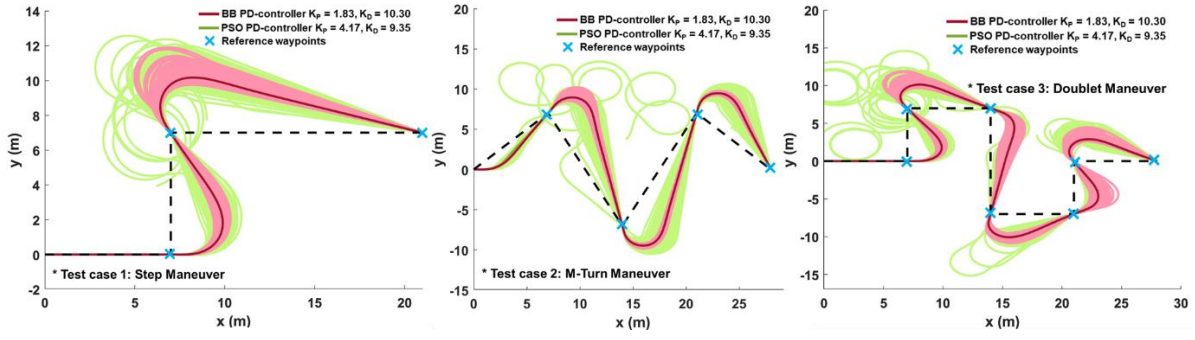

Fig. 8 Step, M-Turn, and Doublet maneuver test cases for 1/80 DTC ship with 20% uncertainty level.

Fig. 8 compares the paths taken by a 1/80 DTC ship controlled by PD-controllers obtained using Bisection Optimization via Blind Search and the Particle Swarm Optimization algorithm. The controller obtained by our proposed method is capable of tracking all of the given reference waypoints. In contrast, the controller obtained from PSO algorithm, which is designed only for nominal parameter values, encounters difficulty when uncertainty introduced.

6. Conclusions

This study designed a fast optimization algorithm to find a robust optimal controller for ship heading angle control with a certain level of error in hydrodynamic coefficients that is difficult to solve deterministically. The optimization error calculation method varied by employing four cost functions: IAE, ISE, ITAE, and ITSE. However, the results in Table 4 show that the optimum controller parameter obtained from different cost functions are insignificant. The addition of a derivative term to the controller, however, resulted in an improved overall system's response. The proposed algorithm works significantly faster than existing methods such as Particle Swarm Optimization (PSO) which compared in Section 4. Our study has several important implications for the field of optimization in dealing with multiple coefficients with some degree of error, like in surface vessels. Having a controller that can compensate for all these uncertainties will make sea sailing and navigation more efficient and safer. Additionally, the robust optimal controllers obtained are pre-processed so that a ship equipped with a less powerful computational processor can implement these controller parameters for higher accuracy and robust control. While our study presents a promising new optimization method for finding robust optimal controller parameters, there are still some limitations that need to be addressed in future research. One limitation is the assumption of undisturbed ship dynamics. Future studies could explore the use of more complex models with disturbances and investigate the effectiveness of our method in dealing with model external uncertainty.

ACKNOWLEDGEMENT

This project was financially supported by Istanbul Technical University (ITU) Scientific Research Projects Coordination Unit Research Fund with Project ID: ITUBAP 44863.

REFERENCES

[1] Song, Z., Ren, G., Mirabella, L., Srivastava, S., 2016. A resilience metric and its calculation for ship automation systems. *2016 Resilience Week (RWS)*, Chicago, USA. https://doi.org/10.1109/RWEEK.2016.7573332

[2] Yoon, H. K., Rhee, K. P., 2003. Identification of hydrodynamic coefficients in ship maneuvering equations of motion by Estimation-Before-Modeling technique. *Ocean Engineering*, 30(18), 2379-2404. https://doi.org/10.1016/S0029-8018(03)00106-9

[3] Sun, N., Wu, Y., Liang, X., Fang, Y., 2019. Nonlinear stable transportation control for double-pendulum shipboard cranes with ship-motion-induced disturbances. *IEEE Transactions on industrial electronics*, 66(12), 9467-9479. https://doi.org/10.1109/TIE.2019.2893855

[4] He, Z., Yuanyuan, H., Cheng, X., Luying, Q., 2021. Model of working ship crossing channel. *Brodogradnja*, 72 (1), 125-143. https://doi.org/10.21278/brod71207

[5] Haseltalab, A., Negenborn, R. R., Lodewijks, G., 2016. Multi-level predictive control for energy management of hybrid ships in the presence of uncertainty and environmental disturbances. *IFAC-PaperOnLine*, 49(3), 90-95. https://doi.org/10.1016/j.ifacol.2016.07.016

[6] Lu, X., Liu, Z., Chu, Z., 2020. Nonlinear adaptive heading control for an underactuated surface vessel with constrained input and sideslip angle compensation. *Brodogradnja*, 71(3), 71-87. https://doi.org/10.21278/brod71305

[7] Chen, X., Tan, W. T., 2013. Tracking control of surface vessels via fault-tolerant adaptive backstepping interval type-2 fuzzy control. *Ocean Engineering*, 70, 97-109. https://doi.org/10.1016/j.oceaneng.2013.05.021

[8] Zhang, Q., Pan, W., Reppa, V., 2022. Model-Reference Reinforcement Learning for Collision-Free Tracking Control of Autonomous Surface Vehicles. *IEEE Transactions on intelligent transportation systems*, 23(7), 8770-8781. https://doi.org/10.1109/TITS.2021.3086033

[9] Ye, J., Roy, S., Godjevac, M., Baldi, S., 2019. Observer-based robust control dynamic positioning of large-scale heavy lift vessels. *IFAC PaperOnLine*, 52(3), 138-143. https://doi.org/10.1016/j.ifacol.2019.06.024

[10] Sariyildiz, E., Oboe, R., Ohnishi, K., 2020. Disturbance Observer-Based Robust Control and Its Applications: 35th Anniversary Overview. *IEEE Transactions on Industrial Electronics*, 67(3), 2042-2053. https://doi.org/10.1016/j.ifacol.2019.06.024

[11] Wang, S., Wang, L., Qiao, Z., Li, F., 2018. Optimal robust control of path following and rudder roll reduction for a container ship in heavy waves. *Applied Science*, 8, 1631. https://doi.org/10.3390/app8091631

[12] Li, Z., Duan, Z., Xie, L., Liu, X., 2012. Distributed robust control of linear multi-agent systems with parameter uncertainties. *International Journal of Control*, 85(8), 1039-1050. https://doi.org/10.1080/00207179.2012.674644

[13] Yasukawa, H., Yoshimura, Y., 2015. Introduction of MMG standard method for ship maneuvering predictions. *Journal of Marine Science and Technology*, 20, 37-52. https://doi.org/10.1007/s00773-014-0293-y

[14] Yao Y., Han L., Wang J., 2018. LSTM-PSO: long short-term memory ship motion prediction based on particle swarm optimization. *IEEE CSAA Guidance, Navigation and Control Conference (CGNCC)*, 1-5. https://doi.org/10.1109/GNCC42960.2018.9018688

[15] Wu, G., Li, Y., Jiang, C., Wang, C., Guo, J., Cheng, R., 2022. Multi-vessels collision avoidance strategy for autonomous surface vehicles based on genetic algorithm in congested port environment. *Brodogradnja*, 73(3), 69-91. https://doi.org/10.21278/brod73305

[16] Helmy, M., Baykaş, T., Arslan, H., 2015. Optimization of aerial base station location in LAP for disaster situations. *IEEE Conference on Standards for Communications and Networking (CSCN)*, Tokyo, Japan. https://doi.org/10.1109/CSCN.2015.7390451

[17] Makhloufi, S., Mekhilef, S., 2022. Logarithmic PSO-based global/local maximum power point tracker for partially shaded photovoltaic systems. *IEEE Journal of Emerging and Selected Topics in Power Electronics*, 10(1), 375-386. https://doi.org/10.1109/JESTPE.2021.3073058

[18] Lu, S., Wang, C., Fan, Y., Lin, B., 2021. Robustness of building energy optimization with uncertainties using deterministic and stochastic methods: Analysis of two forms. *Building and Environment*, 205. https://doi.org/10.1016/j.buildenv.2021.108185

[19] Sabet, M. T., Fathi, A. R., Daniali, M., 2016. Optimal design of the Own Ship maneuver in the bearing-only target motion analysis problem using a heuristically supervised Extended Kalman Filter. *Ocean Engineering*, 123, 146-153. https://doi.org/10.1016/j.oceaneng.2016.07.028

[20] Fridman, E., Shaked, U., 2005. Stability and guaranteed cost control of uncertain discrete delay systems. *International Journal of Control*, 78(4), 235-246. https://doi.org/10.1080/00207170500041472

[21] Keel, L. H., Bhattacharyya, S. P., 1994. Control system design for parametric uncertainty. International *Journal of Robust and Nonlinear Control*, 4, 87-100. https://doi.org/10.1002/rnc.4590040107

[22] Dai, K., Li, Y., 2021. Experimental and numerical investigation on maneuvering performance of small waterplane area twin hull. *Brodogradnja*, 72(2), 93-114. https://doi.org/10.21278/brod72206

[23] Koumboulis, F. N., Tzamtzi, M. P., 2007. A metaheuristic approach for controller design of multivariable processes. *IEEE Conference on Emerging Technologies and Factory Automation (EFTA 2007)*, Patras, Greece. https://doi.org/10.1109/EFTA.2007.4416954

[24] Joseph, S., B., Dada, E. G., Abidemi, A., Oyewola, D. O., Khammas, B. M., 2022. Metaheuristic algorithms for PID controller parameters tuning: review, approaches and open problems. *Heliyon*, 8(5). https://doi.org/10.1016/j.heliyon.2022.e09399

[25] Matusu, R., Pekar, L., 2017. Robust stability of thermal control systems with uncertain parameters: The graphical analysis examples. *Applied Thermal Engineering*, 125, 1157-1163. https://doi.org/10.1016/j.applthermaleng.2017.07.089

[26] Toscano, R., Lyonnet P., 2007. Desing of a robust static output feedback controller in the case of multiple parametric uncertainties. *Transactions of the Institute of Measurement and Control*, 29(1), 71-85. https://doi.org/10.1177/0142331207076371

[27] Khargonekar, P., Tikku, A., 1996. Randomized algorithms for robust control analysis and synthesis have polynomial complexity. *Proceedings of 35th IEEE Conference on Decision and Control*, Kobe, Japan.

[28] Dhanasekaran, B., et al, 2022. Load frequency control assessment of a PSO-PID controller for a standalone multi-source power system. *Technologies*, 11(22). https://doi.org/10.3390/technologies11010022

[29] Mahfoud, S., 2022. Comparative Study between Cost Functions of Genetic Algorithm Used in Direct Torque Control of a Doubly Fed Induction Motor. *Applied Science*, 12, 8717. https://doi.org/10.3390/app12178717

[30] Agrawal, A., 2022. Analytical study of intelligent controller with different objective function to control a complex non-linear system. *13th International Conference on Computing Communication and Networking Technologies (ICCCNT)*, 1-7. https://doi.org/10.1109/ICCCNT54827.2022.9984434

[31] Carrasco D.S., Salgado M.E., 2010. Optimal multivariable controller design using an ITSE performance index. *International Journal of Control*, 83(11), 2340-2353. https://doi.org/10.1080/00207179.2010.520033

[32] Fossen, T. I., Perez, T., 2009. Kalman filtering for positioning and heading control of ships and offshore rigs. *IEEE Control Systems Magazine*, 29(6) 32-46. https://doi.org/10.1109/MCS.2009.934408

[33] Xinyu, L., Renxiang, B., Jiaming, Y., Liangqi, L., Liyuan, S., 2020. Nonlinear modified sliding mode control of ship heading. *7th International Conference on Information Science and Control Engineering (ICISCE)*, Changsha, China. https://doi.org/10.1109/ICISCE50968.2020.00388

Submitted: 28.02.2023.
Accepted: 15.06.2023.

Ahmad Irham Jambak
Department of Mechatronics Engineering, Istanbul Technical University, Istanbul, Turkey
Ismail Bayezit*, bayezit@itu.edu.tr
Department of Mechatronics Engineering, Istanbul Technical University, Istanbul, Turkey
Department of Aeronautical Engineering, Istanbul Technical University, Istanbul, Turkey
Marine Cybernetics Advanced Vehicle Technologies, ITU ARI-Teknokent, Istanbul, Turkey